

Supplementary Information

Sustainable Two-Step Polyelectrolyte Complex for Flame Retardant Nylon-Cotton Fabric

Jovana Petkovska,^a Marija Radoičić,^b Darka Marković,^c Danixa Rodriguez-Melendez,^d Dallin L. Smith,^d Ethan T. Iverson,^d Vesna Dimova,^a Maja Radetić,^e Jaime C. Grunlan,^{*d, f, g} Igor Jordanov^{*a}

^a Faculty of Technology and Metallurgy, Ss. Cyril and Methodius University in Skopje, Ruger Boskovic 16, Skopje 1000, North Macedonia.

^b “Vinča” Institute of Nuclear Sciences, University of Belgrade, Belgrade, Serbia.

^c Innovation Centre of the Faculty of Technology and Metallurgy, University of Belgrade, Karnegijeva 4, Belgrade 11120, Serbia

^d Department of Chemistry, Texas A&M University, College Station, TX 77843, USA.

^e Faculty of Technology and Metallurgy, University of Belgrade, Karnegijeva 4, Belgrade 11120, Serbia.

^f Department of Mechanical Engineering, Texas A&M University, College Station, TX 77843, USA.

^g Department of Materials Science and Engineering, Texas A&M University, College Station, TX 77843, USA.

Table of contents

1. Characterization	3
1.1. <i>Weight gain after single bilayer deposition</i>	3
1.2. <i>Vertical Flame test</i>	3
1.3. <i>Tensile strength and elongation at maximum force</i>	4
1.4. <i>Fabric stiffness</i>	4
1.5. <i>Air permeability</i>	4
1.6. <i>Thermogravimetric analysis</i>	5
1.7. <i>Microscale combustion calorimetry</i>	5
2. Curves obtained from tension tester	6
Fig. S1. Force applied to uncoated and coated samples as a function of their elongation.	6
3. XPS results and spectra analysis	7
Fig. S2. Fitted O 1s spectrum of: a) uncoated and b) 4% EWP ₃ /(1% P-20% GP) ₃ -coated NYCO.....	7
Table S2. Chemical bonds identified in the C 1s spectra with references.	7
Table S3. Chemical bonds identified in the N 1s spectra with references.	7
Table S4. Chemical bond identified in the P 2p and S 2p spectra of 4% EWP ₃ /(1% P-20% GP) ₃ -coated NYCO with references.	7
References	8

1. Characterization

1.1. Weight gain after single bilayer deposition

The NYCO fabric used for coating was cut into strips with dimensions of 80 mm × 350 mm parallel to the warp yarns. Before the coating procedure, the samples were dried at 100 °C for 1 hour and then weighed using a WLC 0.2.X2 analytical and precision balance (Radwag, Poland) to record their initial weight, (weight of the uncoated fabric). After the coating and drying for 1 h at 100 °C, the samples were weighed again (weight of the coated fabric after the single bilayer deposition). The weight gain after single bilayer deposition was calculated using the Equation (S1)

$$\text{Weight gain (\%)} = \frac{m_1 - m_2}{m_1} * 100$$

(S1)

where m_1 is weight of the uncoated fabric and m_2 is the weight of the fabric after the single bilayer deposition.

1.2. Vertical Flame test

The vertical flame test (VFT) was performed following the ASTM D 6413 standard. Before VFT, samples with dimensions 80 mm × 300 mm were weighed using a WLC 0.2.X2 analytical and precision balance (Radwag, Poland). The samples were then mounted on a metal clamp and positioned on the specimen holder inside the FAR FAA4C Flammability Test Chamber (Concept, UK). Each specimen was exposed to a 3 mm high methane flame for 12 seconds, and its behavior during exposure was observed. After the test, the section of the sample covered by the clamp was removed and weighed separately. The residual weight after VFT was calculated using the Equation (S2)

$$\text{Residual weight (\%)} = \frac{m_3}{m_1 - m_2} * 100$$

(S2)

where m_1 is the weight before VFT, m_2 is the weight of the section covered by the clam during VFT, and m_3 is the weight of the remaining part after VFT.

The char length was obtained by measuring the distance from the fabric edge that is directly exposed to the flame to the farthest point of visible damage caused by the flame. The maximum char width is obtained by measuring the widest part of the charred area.

The burning rate of the samples that do not self-extinguish during the 12 seconds of flame exposure was calculated using Equation (S3)

$$\text{Burning rate (mm/s)} = \frac{l}{t} \quad (\text{S3})$$

where l is the length of the sample in mm before VFT and t is the recorded burning time in seconds after the 12 s of flame exposure.

1.3. Tensile strength and elongation at maximum force

Tensile strength and elongation at maximum force were measured using the Tinus Olsen tension tester H5KT (Salfords, UK). The textile tensile properties were measured according to the EN ISO 13934-1 standard- Part 1: Determination of maximum force and elongation using the strip method. Fabric strips measuring 50 mm in width and 200 mm in length were mounted between two clamps, set 200 mm apart. The testing conditions included a constant elongation rate of 100 mm/min and a pretension of 5 N. During the test, tensile strength (in N), elongation at maximum force (expressed as a percentage), and force-elongation curves were recorded.

1.4. Fabric stiffness

Fabric stiffness was assessed using the SDL Atlas digital pneumatic stiffness tester (Rock Hill, South Carolina, USA) following the ASTM D 4032-94 standard for fabric stiffness by the circular bend procedure. Each specimen was folded to form a square with dimensions 102 mm x 102 mm and placed on the testing platform. A plunger with a diameter of 25.4 mm, equipped with a pneumatic actuator set to an air pressure of 324 kPa, was used to push the fabric through an orifice with a diameter of 38 mm. The maximum force needed to push the fabric through the orifice was recorded in N and referred to as the Stiffness Force.

1.5. Air permeability

The air permeability was evaluated using the AirPerm Air Permeability Tester (SDL Atlas, Rock Hill, South Carolina, USA) according to the ISO 9237:1995 standard, with a test surface area of

20 cm² and a pressure drop of 100 Pa for both uncoated and coated NYCO. Each specimen with dimensions of 80 mm in width and 300 mm in length was tested for air permeability at three different points along its length, with the results recorded in mm/s.

1.6. Thermogravimetric analysis

Thermogravimetric analysis was performed using a Linseis STA PT 1000 thermogravimetric analyzer (Linseis Messgeraete GmbH, Selb, Germany). An alumina crucible was used to hold the sample during the analysis. Approximately 5 mg of sample was heated from ambient temperature to 700 °C at a rate of 10 °C/min, with measurements conducted in an air atmosphere at a flow rate of 100 mL/min for the sample gas and 50 mL/min for the nitrogen purge gas. For nitrogen measurements, both sample and purge gases were nitrogen, with flow rates of 100 and 50 mL/min, respectively. The collected data was evaluated using the Linseis Platinum Software.

1.7. Microscale combustion calorimetry

Microscale combustion calorimetry (MCC) was carried out using a microscale combustion calorimeter MCC-3 (Deatak, McHenry, IL), following the Method A of the ASTM D7309 standard. Approximately 5 mg of sample was heated at 1 °C/sec to 600°C under nitrogen with flow rate of 80 mL/min. The thermal degradation products were mixed with a 20 mL/min stream of oxygen before entering a 900 °C combustion furnace. The collected data was evaluated using the MCC software provided by the manufacturer.

2. Curves obtained from tension tester

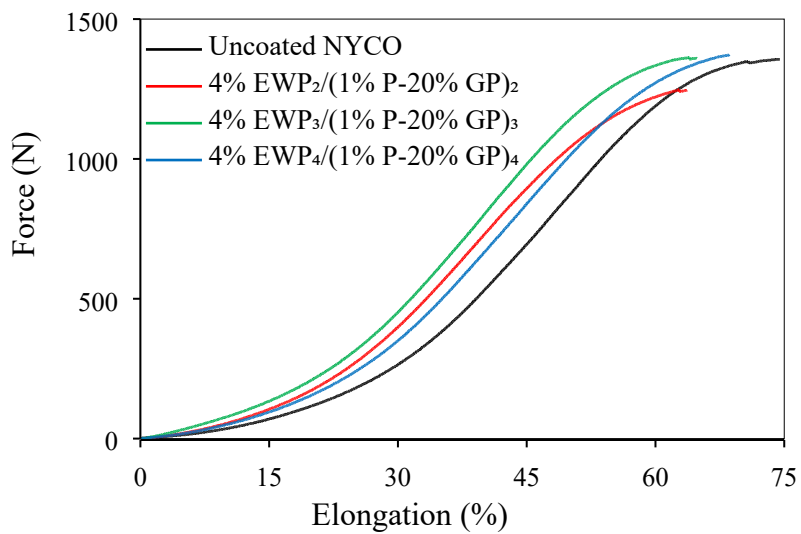


Fig. S1. Force applied to uncoated and coated samples as a function of their elongation.

3. XPS results and spectra analysis

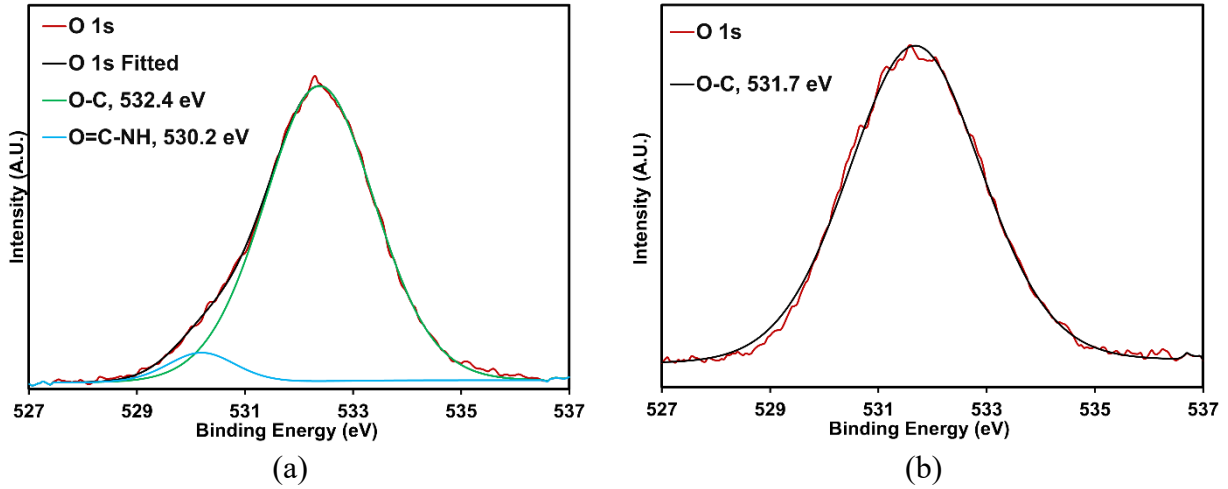


Fig. S2. Fitted O 1s spectrum of: a) uncoated and b) 4% EWP₃/(1% P-20% GP)₃-coated NYCO.

Table S1. Chemical bonds identified in the O 1s spectra with references.

Chemical bond	Binding energy (eV)		Reference
	Uncoated NYCO	4% EWP ₃ /(1% P-20% GP) ₃	
O-C	532.4	531.7	(Thota et al., 2020)
O=C-NH	530.2	N/A	

Table S2. Chemical bonds identified in the C 1s spectra with references.

Chemical bond	Binding energy (eV)		Reference
	Uncoated NYCO	4% EWP ₃ /(1% P-20% GP) ₃	
C-C	283.9	284.7	(Thota et al., 2020)
C-N	285.5	286.0	
C-O	286.5	N/A	
C=O	N/A	287.9	(Arshad et al., 2021)

Table S3. Chemical bonds identified in the N 1s spectra with references.

Chemical bond	Binding energy (eV)		Reference
	Uncoated NYCO	4% EWP ₃ /(1% P-20% GP) ₃	
N-C	399.2	399.5	(Lee et al., 2016)
N=C	N/A	400.7	(Battirola et al., 2018)

Table S4. Chemical bond identified in the P 2p and S 2p spectra of 4% EWP₃/(1% P-20% GP)₃-coated NYCO with references.

Chemical bond	Binding energy (eV)	Reference
P-O	133.2	(Li et al., 2013)
S-C	163.6	(Wu et al., 2019)
S=O	167.4	(Kim et al., 2018)

References

- Arshad, N., Sultan Irshad, M., Sehar Abbasi, M., Rehman, S.U., Ahmed, I., Qasim Javed, M., Ahmad, S., Sharaf, M., Firdausi, M.D.A., 2021. Green thin film for stable electrical switching in a low-cost washable memory device: proof of concept. *RSC Adv.* 11, 4327–4338. <https://doi.org/10.1039/D0RA08784J>
- Battirola, L.C., Rudolf, P., Tremiliosi-Filho, G., Rodrigues-Filho, U.P., 2018. Thermally induced chemical evolution in polyimide films investigated by X-ray photoelectron spectroscopy. *Polym. Eng. Sci.* 58, 943–951. <https://doi.org/10.1002/pen.24649>
- Kim, S.S., Britcher, L., Kumar, S., Griesser, H.J., 2018. XPS Study of Sulfur and Phosphorus Compounds with Different Oxidation States. *Sains Malays.* 47, 1913–1922. <https://doi.org/10.17576/jsm-2018-4708-33>
- Lee, K.M., Kim, M., Lee, E., Baeck, S.H., Shim, S.E., 2016. Nylon 6,6/Polyaniline Based Sheath Nanofibers for High-Performance Supercapacitors. *Electrochimica Acta* 213, 124–131. <https://doi.org/10.1016/j.electacta.2016.07.104>
- Li, R., Wei, Z., Gou, X., Xu, W., 2013. Phosphorus-doped graphene nanosheets as efficient metal-free oxygen reduction electrocatalysts. *RSC Adv.* 3, 9978–9984. <https://doi.org/10.1039/C3RA41079J>
- Thota, S., Somiseti, V., Kulkarni, S., Kumar, J., Nagarajan, R., Mosurkal, R., 2020. Covalent functionalization of cellulose in cotton and a nylon-cotton blend with phytic acid for flame retardant properties. *Cellulose* 27, 11–24. <https://doi.org/10.1007/s10570-019-02801-6>
- Wu, T., Jing, M., Yang, L., Zou, G., Hou, H., Zhang, Yang, Zhang, Yu, Cao, X., Ji, X., 2019. Controllable Chain-Length for Covalent Sulfur–Carbon Materials Enabling Stable and High-Capacity Sodium Storage. *Adv. Energy Mater.* 9, 1803478. <https://doi.org/10.1002/aenm.201803478>